Journal of Alloys and Compounds 504 (2010) 22–26

Contents lists available at ScienceDirect

Journal of Alloys and Compounds

journal homepage: www.elsevier.com/locate/jallcom

Dependence of energy transfer and photoluminescence on tailored defects in Eu-doped ZnO nanosheets-based microflowers

D.D. Wang[a,b,c,d,*], G.Z. Xing[d,e], J.H. Yang[a,**], L.L. Yang[a], M. Gao[a], J. Cao[b,c], Y.J. Zhang[a], B. Yao[e]

[a] Institute of Condensed Matter Physics, Jilin Normal University, Siping, 136000, PR China
[b] Key Laboratory of Excited State Processes, Changchun Institute of Optics, Fine Mechanics and Physics Chinese Academy of Sciences, Changchun, 130033, PR China
[c] Graduate School of the Chinese Academy of Sciences, Beijing, 100049, PR China
[d] Division of Physics and Applied Physics, School of Physical and Mathematical Sciences, Nanyang Technological University, Singapore, 637371, Singapore
[e] Department of Physics, Jilin University, Changchun 130023, PR China

ARTICLE INFO

Article history:
Received 1 January 2010
Received in revised form 17 May 2010
Accepted 22 May 2010
Available online 4 June 2010

Keywords:
Oxide materials
Rare earth
Chemical synthesis
Optical properties

ABSTRACT

Eu-doped ZnO nanosheets-based microflowers have been synthesized successfully by using a hydrothermal method. Eu^{3+}-related red emission results from energy transfer are observed in the microflowers under UV laser excitation. Further systematic photoluminescence studies on the samples upon oxygen and vacuum annealing treatments suggest that there exists a strong correlation between the intrinsic defects and the efficiency of the Eu^{3+}-related emission. It is demonstrated that these defects may act as the media in the energy transfer process from the ZnO host to Eu^{3+} ions.

1. Introduction

Recently, rare-earth (RE) doped-VI semiconductors have received significant attention due to their applications in optoelectronic devices [1–3]. Trivalent RE^{3+} ions exhibit very sharp and temperature independent RE intra-4f shell transitions, since the 4f shell is well shielded by the outer 5s and 5p electrons. The use of a semiconductor host enables minority carrier injection to excite RE 4f shell electrons, resulting in 4f shell luminescence. ZnO is a wide bandgap II–VI semiconductor (3.37 eV) [4]. It is economical, environmental friendly, and exhibits high thermal and chemical stability [5–7]. Importantly, it has a large exciton binding energy of 60 meV [7,8] which is much higher than the thermal energy at room temperature (RT). These properties make it a unique host material for doping with luminescence centers and it can exhibit efficient emission even at or above RT. There have been many reports on the UV, blue and green emissions from ZnO [9–11], but the systematic investigation on the intense red emission of ZnO is limited. Among the RE^{3+} activators, the red $^5D_0$–$^7F_2$ emission of Eu^{3+} is widely explored in light-emitting devices. Recently, there have been many reports focusing on Eu-doped ZnO materials [12–14]. However, even after doping is confirmed in some previous reports, there is still no efficient red emission reported in Eu-doped ZnO. Because the luminescence lifetime of RE ions is in the micro and milli-second time scale, 10^2 times slower than decay of excitons in ZnO, and this mismatch makes direct energy transfer from ZnO to RE ions very impossible [15]. Furthermore, the quenching effect on RE emission appears due to the self-activated transitions in the ZnO matrix [16]. Fortunately, energy transfer can be facilitated by the presence of intrinsic or extrinsic defects as energy trapping centers in various systems, such as SiC:(N, Er), ZnO:(N, Eu) and ZnO:(F, Eu) [17,18], which suggest that the introduction of the appropriate trap centers is crucial for efficient ZnO → Eu^{3+} energy transfer. Park et al. reported that chlorine impurities can assist red emission in Eu^{3+}-doped ZnO [13,16]. In a recent work, Zeng et al. claimed that Eu^{2+} ions act as trapping centers in Eu-doped ZnO microflowers and transfer energy to the Eu^{3+} ions [19], consequently leading to red emission. Wang et al. indicated that the surface defects may dedicate the process of energy transfer from ZnO to Eu^{3+} ions [20]. However, there have been no systematic studies on defects engineering upon the energy transfer efficiency in Eu-doped ZnO system.

In present work, we fabricated Eu-doped ZnO nanosheets-based microflowers via a hydrothermal method. We observed the effi-

* Corresponding author at: Institute of Condensed Matter Physics, Jilin Normal University, Siping, 136000, PR China. Fax: +86 3294566.
** Corresponding author at: Institute of Condensed Matter Physics, Jilin Normal University, Siping, 136000, PR China. Fax: +86 3290009.
E-mail addresses: ddwang@ntu.edu.sg (D.D. Wang), jhyang@jlnu.edu.cn (Y.J. Zhang).

0925-8388/$ – see front matter © 2010 Elsevier B.V. All rights reserved.
doi:10.1016/j.jallcom.2010.05.105

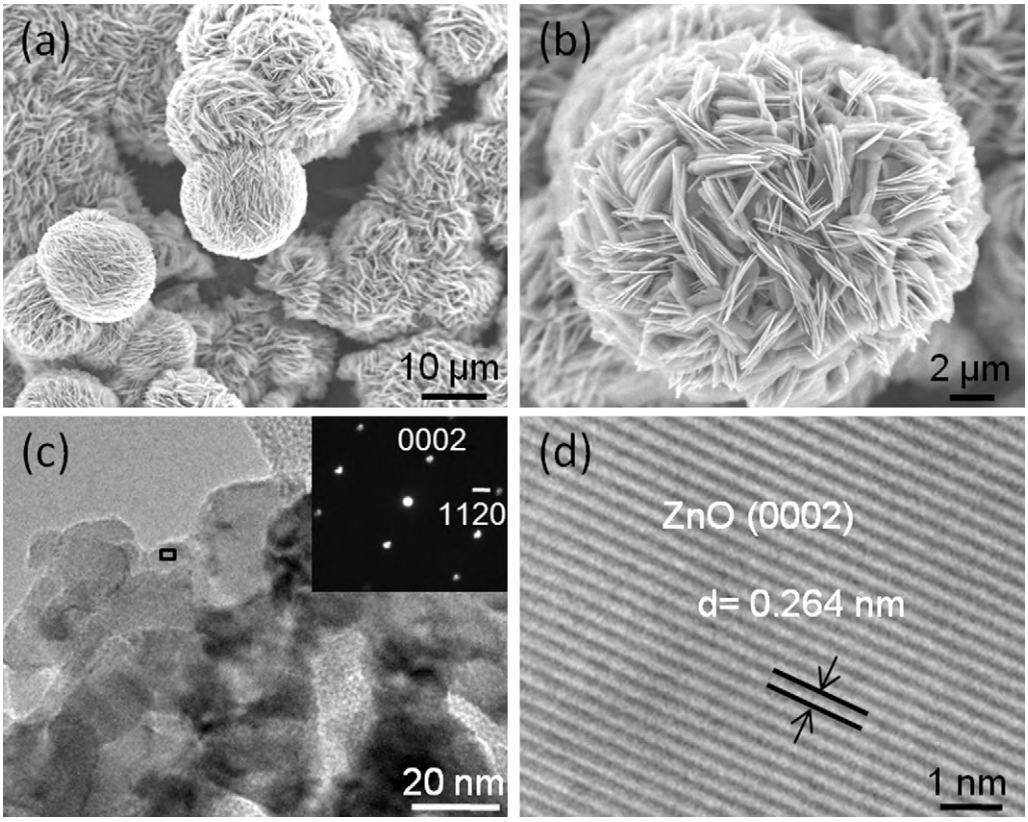

Fig. 1. (a) Low- and (b) high-magnification FESEM images of EZO-AS. (c) Transmission electron microscopy image of the nanosheets in EZO-AS. (d) High resolution TEM image and inset of (c) shows the corresponding SAED patterns.

cient sharp red emission from Eu^{3+} ions excited by the energy from ZnO host. Systematic studies of photoluminescence (PL) of the samples through different annealing treatments suggest that the intrinsic defects can serve as media for the energy transfer from ZnO host to Eu^{3+} ions.

2. Experimental

Eu-doped ZnO nanosheets-based microflowers were synthesized by the hydrothermal method accompanied with the different post-synthesis heat treatments. $Zn(NO_3)_2{\cdot}6H_2O$ was dissolved in deionized water. Eu_2O_3 powder was dissolved in dilute nitric acid to obtain a 0.01 M europium nitrate aqueous solution. The two solutions were mixed and urea added with a molar ratio of Zn:Eu:urea of 1:0.02:10, and the concentration of the metal ions in solution was adjusted to 0.01 M (pH ≈ 6). After stirring, the solution was transferred into a 100 ml Teflon-lined autoclave, which was filled to nearly 80% of its capacity. The autoclave was kept in a dry cabinet at 120 °C for 6 h, then the solution was cooled down to RT. White powder collected from the bottom of the container was washed with ethanol and distilled water, and then dried at 60 °C and annealed at 400 °C in air for 2 h. Herein, we name the as-grown sample as EZO-AS. Two more kinds of sample were obtained with different post annealing treatments: (i) oxygen annealing at 550 °C for 0.5 h (sample EZO-O); (ii) vacuum (1.0×10^{-3} Pa) annealing at 550 °C for 0.5 h (sample EZO-V). For comparison, the undoped ZnO samples (UZO) were also synthesized with the identical experimental conditions except that the Eu_2O_3 was not used in the source. The crystal structure and morphology of the samples were studied by X-ray diffractometer (XRD), transmission electron microscopy (TEM (JOEL 2100) and JOEL JSM-6700F field emission scanning electron microscope (FESEM). A quantitative compositional analysis was conducted by using an X-ray photoelectron spectroscopy (XPS) in an ultra-high-vacuum chamber at a pressure lower than 1.0×10^{-9} Torr. RT PL was characterized by He–Cd laser with a 325 nm excitation line. The excitation and emission spectra were taken at RT on a Hitachi F-4500 spectrofluorimeter equipped with a 150-W xenon lamp as excitation source.

3. Results and discussion

Fig. 1a and b shows the FESEM images of EZO-AS appearing as uniform microflowers, and their average diameter is about 15 μm. Each microflower is composed of many ultrafine nanosheets. The thickness of the nanosheets is about 80 nm. Some microflowers connect with each other. TEM and selected area electron diffraction (SAED) patterns in Fig. 1c and d indicate that the nanosheet exhibits large single crystal mesoporous sheet and grow along the [0 0 0 1] direction as other ZnO nanostructures [21], and no secondary phase or impurity was observed.

The XRD pattern of EZO-AS shown in Fig. 2a can be indexed consistently with crystalline wurtzite ZnO structure. No any other phase such as europium oxide was detected within the detection limit. To investigate the chemical composition and bonding states, XPS experiments were performed on EZO-AS. Prior to XPS measurements, samples were sputtered by Ar ions to remove any potential surface contamination [22,23]. A typical XPS survey scan is shown in Fig. 2b. The survey scan confirms the presence of Zn, O, Eu and C and the absence of other impurities. Fig. 2c-e illustrate the core-level XPS spectra of O 1s, Zn 2p and Eu 3d, respectively. Fitting of O peaks indicates that two species of oxygen are present as shown in Fig. 2c. The peak at 530.2 eV is attributed to O^{2-} ions on wurtzite structure of hexagonal Zn^{2+} ion matrix, surrounded by Zn atoms, while the peak at 531.2 eV usually originated from chemisorbed oxygen on the nanosheets surface [24]. In Fig. 2d, two peaks at 1044.8 and 1021.5 eV were ascribed to the core levels of Zn $2p_{1/2}$ and Zn $2p_{3/2}$ of ZnO, respectively. In Fig. 2e, the peaks at 1135.1 and 1165.5 eV correspond to Eu $3d_{5/2}$ and Eu $3d_{3/2}$, respectively [25]. Their positions indicate that the Eu ion has a +3 valence in Eu-doped ZnO nanosheets-based microflowers [26]. By fitting the integrated peak areas and using the calibrated atomic sensitivity factors, the atomic ratio of Eu to Zn was quantitatively determined to be ~0.009.

The systematic optical measurements were carried out on the sample EZO-AS. In Fig. 3a, it exhibits a weak UV emission attributed

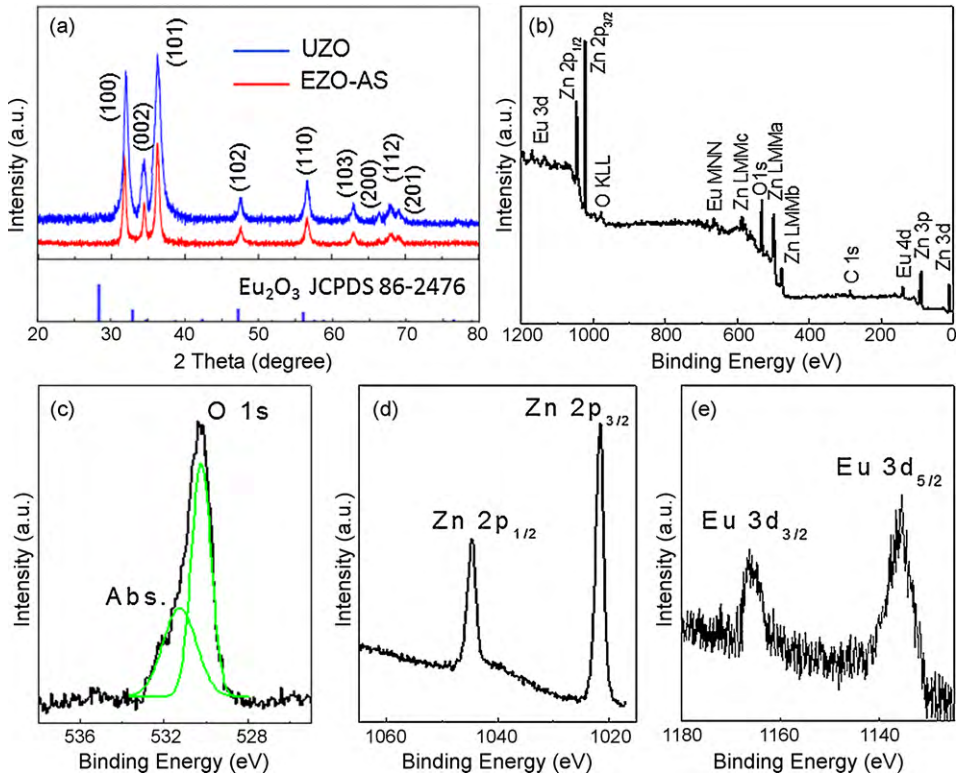

Fig. 2. (a) XRD patterns of EZO-AS and UZO. (b) XPS survey spectrum of EZO-AS. (c) O 1s, (d) Zn 2p, (e) Eu 3d detailed scan recorded for EZO-AS.

to near-band-edge (NBE) exciton recombination [27], and a broad deep level emission (DLE) from 450 to 700 nm ascribed to defects level related transition [28–30]. In addition, a sharp red emission peak appears riding on DLE band. Due to the asymmetry of the broad DLE band, we fitted it into two emission bands: weak green band (centered on ~520 nm) and strong yellow-orange band (centered on ~610 nm). The DLE band has previously been attributed to different defects in ZnO such as O-vacancy (V_O) [31–33], Zn-vacancy (V_{Zn}) [34–36], O-interstitial (O_i) [37], Zn-interstitial (Zn_i) [38], and extrinsic impurities such as substitutional Cu [39]. For the green emission, though a number of hypotheses have been proposed, some assignments are highly controversial. Typical works reported that the transitions may occur between singly ionized oxygen vacancies and photoexcited holes, or electrons close to the conductive band and deeply trapped holes at V_O^{2+}, anitiste oxygen, zinc interstitials, zinc vacancies, *etc.* [40]. The yellow–orange band emission is attributed to the oxygen interstitial defects located in the bulk [41]. The sharp red emission results from the intra-4f transition of Eu^{3+} ions [42]. The intensity of red emission is comparable to intrinsic defect emission. This indicates that there is efficient energy transfer from ZnO host to Eu^{3+} ions [19]. Moreover, in the excitation spectra (Fig. 3b), a strong excitation peak appears at UV range that corresponds to the transition from valence band (VB) to conduction band (CB) of ZnO, which confirms the energy transfer from UV-generated delocalized electron and hole pairs in ZnO host to Eu^{3+} ions. Other excitation peaks at 393, 413, 465 and 538 nm are likely originated from the $^7F_0$–$^5L_6$, and $^7F_0$–^5D_J (J = 3, 2, 1) transition of Eu^{3+} ions [43]. In addition, the PL properties under resonant (465 nm) excitations were also investigated and shown in Fig. 3c. Emission peaks are attributed to the $^5D_0$–^7F_J (J = 1, 2, 3, 4) transitions [44].

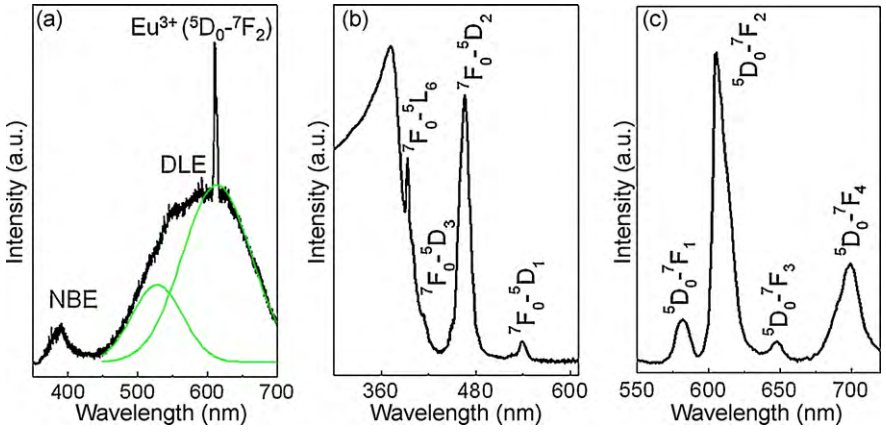

Fig. 3. (a) Emission spectrum of EZO-AS under 325 nm excitation wavelength. (b) Excitation spectrum of EZO-AS, monitored at 615 nm. (c) Emission spectrum of EZO-AS under 465 nm excitation wavelength.

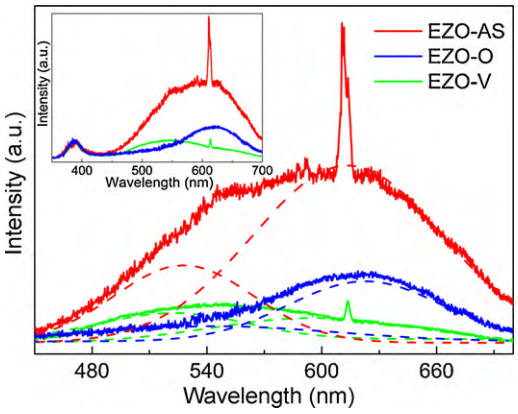

Fig. 4. Emission spectra of EZO-AS with different annealing treatments under 325 nm excitation wavelength. Inset shows the full spectra of samples.

The PL properties of Eu-doped ZnO nanosheets-based microflowers subjected to annealing in different atmospheres were investigated and shown in Fig. 4. The inset is the full PL spectra of samples. All PL spectra were normalized by intensity of UV emission. Each broad defect emission was fitted with Gaussian functions to identify two main emissions. The intensities of defect emissions are all reduced due to enhancement of crystal quality after annealing. However, the different post annealing methods have distinct effects on the defect emission. Compared with the results of sample annealed under vacuum atmosphere (EZO-V), the green emission weakened considerably in sample EZO-O. And in EZO-V the green emission dominates the broad defect emissions due to the yellow emission center (oxygen interstitial) outdiffuse from interstitial site of Eu-doped ZnO after vacuum annealing. Interestingly, the sharp red emission disappears when green emission becomes very weak in EZO-O, whereas still present in EZO-V. The red emission has the same trend with the green emission under different post annealing: when the intensity of green emission becomes the strongest one, the red emission intensity is also highest one. In general, transfer of the excitation energy from the host to the doping ions is inefficient, and most of the energy is released through these channels, such as multiple phonon non-radiative transitions, bound excitons and self-activated centers [18]. However, if one produces certain defects as trapping and energy storage centers, energy transfer can substantially enhanced [18,45]. In ZnO, the energy level of defects related to green emission is 2.3–2.45 eV [46], which is close to the excited state energy of Eu^{3+}, thus non-radiative energy transfer from these defects to Eu^{3+} ions is favorable. Defects related to green emission act as the energy storage centers in the energy transfer process. We are currently conducting the temperature-dependent and excitation-dependent PL to further investigate the type of defects which may act as the media during the energy transfer process in Eu-doped ZnO samples.

4. Conclusions

In summary, Eu-doped ZnO microflowers were synthesized by using a facile hydrothermal method. We observed the intra 4f emission of Eu^{3+} due to the energy transfer from ZnO host to Eu^{3+} ions. After the oxygen and vacuum annealing, it is found that the red and green emissions behave the same trend subjected to different atmosphere treatments. It indicates that there is a strong correlation between the defects related green emission and the characteristics of the Eu^{3+}-related red emission, which suggests that the intrinsic defects can assist efficient energy transfer from the ZnO host to the Eu^{3+} ions. This study suggests that defect engineering is a viable approach to exploit ZnO-based nanomaterials in optoelectronic and display applications.

Acknowledgements

This work was supported by the Singapore Ministry of Education Research grants (SUG 20/06, RG 46/07 and SUG M58110068), the program of National Natural Science Foundation of China (no. 60778040 and 60878039), the National Youth Program Foundation of China (grant no. 10904050), gifted youth program of Jilin province (no. 20070118), the Science and Technology Bureau of Key Program for Ministry of Education (item no. 207025), 2007 introduction of foreign technology, project management talents (item no. S20072200001). G.Z. Xing acknowledges the financial support of Singapore Millennium Foundation Scholarship, Singapore.

References

[1] A.A. Bol, R. van Beek, A. Meijerink, Chem. Mater. 14 (2002) 1121.
[2] X. Wang, X.G. Kong, G.Y. Shan, Y. Yu, Y.J. Sun, L.Y. Feng, K.F. Chao, S.Z. Lu, Y.J. Li, J. Phys. Chem. B 108 (2004) 18408.
[3] A.S. Pereira, M. Peres, M.J. Soares, E. Alves, A. Neves, T. Monteiro, T. Trindade, Nanotechnology 17 (2006) 834.
[4] L. Liao, B. Yan, Z. Zhang, L.L. Chen, B.S. Li, G.Z. Xing, Z.X. Shen, T. Wu, X.W. Sun, J. Wang, T. Yu, ACS Nano 3 (2009) 700.
[5] G.Z. Xing, J.B. Yi, J.G. Tao, T. Liu, L.M. Wong, Z. Zhang, G.P. Li, S.J. Wang, J. Ding, T.C. Sum, C.H.A. Huan, T. Wu, Adv. Mater. 20 (2008) 3521.
[6] J.H. Yang, D.D. Wang, L.L. Yang, Y.J. Zhang, G.Z. Xing, J.H. Lang, H.G. Fan, M. Gao, Y.X. Wang, J. Alloys Compd. 450 (2008) 508.
[7] T. Chen, G.Z. Xing, Z. Zhang, H.Y. Chen, T. Wu, Nanotechnology 19 (2008) 435711.
[8] G.Z. Xing, B. Yao, C.X. Cong, T. Yang, Y.P. Xie, B.H. Li, D.Z. Shen, J. Alloys Compd. 457 (2008) 36.
[9] Ü. Özgür, Y.I. Alivov, C. Liu, A. Teke, M.A. Reshchikov, S. Doğan, V. Avrutin, S.J. Cho, H. Morkoc, J. Appl. Phys. 98 (2005) 041301.
[10] X.M. Zhang, M.Y. Lu, Y. Zhang, L.J. Chen, Z.L. Wang, Adv. Mater. 21 (2009) 1.
[11] M.H. Huang, S. Mao, H. Feick, H.Q. Yan, Y.Y. Wu, H. Kind, E. Weber, R. Russo, P.D. Yang, Science 292 (2001) 1897.
[12] C.C. Yang, S.Y. Cheng, H.Y. Lee, S.Y. Chen, Ceram. Int. 32 (2006) 37.
[13] Y.K. Park, J.I. Han, M.G. Kwak, H. Yang, S.H. Ju, W.S. Cho, Appl. Phys. Lett. 72 (1998) 668.
[14] Y. Hayashi, H. Narahara, T. Uchida, T. Noguchi, S. Ibuki, Jpn. J. Appl. Phys. 34 (1995) 1878.
[15] A. Van Dijken, E.A. Meulenkamp, D. Vanmaekelbergh, A. Meijerink, J. Lumin. 87 (2000) 454.
[16] Y.K. Park, J.I. Han, M.G. Kwak, H. Yang, J. Sung Hoo, W.S. Cho, J. Lumin. 78 (1998) 87.
[17] D. Prezzi, T.A.G. Eberlein, J.S. Filhol, R. Jones, M.J. Shaw, P.R. Briddon, S. Oberg, Phys. Rev. B 69 (2004) 193202.
[18] W.Y. Jia, K. Monge, F. Fernandez, Opt. Mater. 23 (2003) 27.
[19] X.Y. Zeng, J.L. Yuan, Z.Y. Wang, L. Zhang, Adv. Mater. 19 (2007) 4510.
[20] M. Wang, C. Huang, Z. Huang, W. Guo, J. Huang, H. He, H. Wang, Y. Cao, Q. Liu, J. Liang, Opt. Mater. 31 (2009) 1502.
[21] G.Z. Xing, J.G. Tao, G.P. Li, Z. Zhang, L.M. Wong, S.J. Wang, C.H.A. Huan, T. Wu, 2008 2nd IEEE International Nanoelectronics Conference, vol. 1–3, 2008, p. 462.
[22] D.D. Wang, G.Z. Xing, H.Y. Peng, T. Wu, J. Phys. Chem. C 113 (2009) 7065.
[23] G.Z. Xing, J.B. Yi, D.D. Wang, L. Liao, T. Yu, Z.X. Shen, C.H.A. Huan, T.C. Sum, J. Ding, T. Wu, Phys. Rev. B 79 (2009) 174406.
[24] L.J. Meng, C.P. Moreira, M.P.D. Santos, Appl. Surf. Sci. 78 (1994) 57.
[25] X.L. Tan, X.K. Wang, H. Geckeis, T.H. Rabung, Environ. Sci. Technol. 42 (2008) 6532.
[26] R. Vercaemst, D. Poelman, L. Fiermans, R.L. Van Meirhaeghe, W.H. Laflere, F. Cardon, J. Electron. Spectrosc. Relat. Phenom. 74 (1995) 45.
[27] D.D. Wang, J.H. Yang, G.Z. Xing, L.L. Yang, J.H. Lang, M. Gao, B. Yao, T. Wu, J. Lumin. 129 (2009) 996.
[28] G.Z. Xing, D.D. Wang, J.B. Yi, L.L. Yang, M. Gao, M. He, J.H. Yang, Q.X. Zhao, J. Ding, T.C. Sum, T. Wu, Appl. Phys. Lett. 96 (2010) 112511.
[29] H.B. Lu, H. Li, L. Liao, Y. Tian, M. Shuai, J.C. Li, M.F. Hu, Q. Fu, B.P. Zhu, Nanotechnology 19 (2008) 045605.
[30] H.B. Lu, L. Liao, J.C. Li, D. Wang, H. He, Q. Fu, L. Xu, Y. Tian, J. Phys. Chem. B 110 (2006) 23211.
[31] P.H. Kasai, Phys. Rev. 130 (1963) 989.
[32] S. Yamauchi, Y. Goto, T. Hariu, J. Cryst. Growth 260 (2004) 1.
[33] D.D. Wang, J.H. Yang, L.L. Yang, Y.J. Zhang, J.H. Lang, M. Gao, Cryst. Res. Technol. 43 (2009) 1041.
[34] M. Liu, A.H. Kitai, P. Mascher, J. Lumin. 54 (1992) 35.
[35] E.G. Bylander, J. Appl. Phys. 49 (1978) 1188.

[36] X. Yang, G. Du, X. Wang, J. Wang, B. Liu, Y. Zhang, D. Liu, D. Liu, H.C. Ong, S. Yang, J. Cryst. Growth 252 (2003) 275.
[37] J. Zhong, A.H. Kitai, P. Mascher, W. Puff, J. Electrochem. Soc. 140 (1993) 3644.
[38] K. Johnston, M.O. Henry, D.M. Cabe, T. Agne, T. Wichert, Proceedings of the Second Workshop on SOXESS European Network on ZnO, 27–30 October, Caernarfon, Wales, UK, 2004.
[39] R. Dingle, Phys. Rev. Lett. 23 (1969) 579.
[40] M.A. Reshchikov, H. Morkoc, B. Nemeth, J. Nause, J. Xie, B. Hertog, A. Osinsky, Physica B 401–402 (2007) 358–361.
[41] D. Li, Y.H. Leung, A.B. Djurišić, Z.T. Liu, M.H. Xie, S.L. Shi, S.J. Xu, W.K. Chan, Appl. Phys. Lett. 85 (2004) 1601.
[42] S. Sadhu, T. Sen, A. Patra, Chem. Phys. Lett. 440 (2007) 121.
[43] Y.S. Liu, W.Q. Luo, R.F. Li, X.Y. Chen, Opt. Lett. 32 (2007) 566.
[44] Y.P. Du, Y.W. Zhang, L.D. Sun, C.H. Yan, J. Phys. Chem. C 112 (2008) 12234.
[45] X. Zeng, J. Yuan, L. Zhang, J. Phys. Chem. C 112 (2008) 3503.
[46] K. Vanheusden, W.L. Warren, C.H. Seager, D.R. Tallant, J.A. Voigt, B.E. Gnade, J. Appl. Phys. 79 (1996) 7983.